ECG Artefact Identification and Removal in mHealth Systems for Continuous Patient Monitoring

Syed Anas Imtiaz, James Mardell, Siavash Saremi–Yarahmadi and Esther Rodriguez–Villegas

Department of Electrical and Electronic Engineering, Imperial College London, SW7 2AZ, UK

Submission for *mHealth – Emerging Mobile Health Systems and Services* Special Issue in Healthcare Technology Letters.

Continuous patient monitoring systems acquire enormous amounts of data that is either manually analysed by doctors or automatically processed using intelligent algorithms. Sections of data acquired over long period of time can be corrupted with artefacts due to patient movement, sensor placement and interference from other sources. Because of the large volume of data these artefacts need to be automatically identified so that the analysis systems and doctors are aware of them while making medical diagnosis. This paper explores three important factors that must be considered and quantified for the design and evaluation of automatic artefact identification algorithms: signal quality, interpretation quality and computational complexity. The first two are useful to determine the effectiveness of an algorithm while the third is particularly vital in mHealth systems where computational resources are heavily constrained. A series of artefact identification and filtering algorithms are then presented focusing on the electrocardiography data. These algorithms are quantified using the three metrics to demonstrate how different algorithms can be evaluated and compared to select the best ones for a given wireless sensor network.

1. Introduction: The mainstream use of smartphones and the miniaturization of electronics has led to widespread availability of various smart and wireless sensors for continuous healthcare monitoring. These sensors acquire relevant signals and transmit them wirelessly to a smartphone or a base station that can run some diagnostic algorithms or transmit them via internet for further analysis. Although this trend is highly useful allowing patients to have multiple wearable sensors enabling different physiological measurements simultaneously, the abundance of these monitoring sensors has led to significant problems in data acquisition and management. The large quantity of data acquired by multiple sensors places substantial demands on the medical profession as well as the receiving infrastructure. Traditional methods for mitigating this problem include intermittent recording, compression and manual analysis. However, with a plethora of data sources continuously acquiring data, these methods are no longer suitable. Therefore automatic analysis algorithms are used to sift through this large quantity of data which would otherwise take several hours or days for manual analysis.

Algorithms for automated analysis of signals are heavily dependent on the quality of signals that are recorded. Hence, providing reliable data to the analysis system is pivotal for meaningful alerts and diagnoses to occur. This data may be affected by several sources of noise and movement artefacts. These artefacts are even more likely to be present when signals are continuously acquired over long periods of time using wearable sensors, that allow patient mobility, compared to the in-hospital acqusition systems that are very well controlled.

This paper attempts to solve some of the issues associated with the quality of data acquired using wearable sensors. It looks at identification of problems that could impact the data quality, affecting the automated analysis of these physiological signals. As a result, corrupted signals can be marked automatically informing the physicians of their unreliability.

Although this problem is true for all healthcare devices that are used for long-term monitoring, the work presented in this paper is part of a larger project for smart diabetes management [1]. It is well known that patients with diabetes, in particular, devote a large amount of their time to the management and acquisition of data [2]. A smart diabetes management system can thus notify medical professionals of its findings and assist them in providing care to diabetic patients. Fundamental to the entire system working is the recording of several physiological signals from the wearable sensors used by the patient. In recent years there has been a large number of such wearable body monitoring sensors available that can be used for the diabetes management system. However, the data recorded by these devices can be corrupted with artefacts and difficult to manage because of its large volume. Further, the system itself should remain sensor-agnostic, and be independent of the exact model or make of the sensor used. For the aforementioned diabetes management system, the *Zephyr BioHarness 3* [3] was used for data collection. The suitability of the *BioHarness 3* for the continuous monitoring of clinical trial patients was determined by its small size, weight, ease of application and robust wireless transmission of electrocardiography, respiratory and movement sensor data. However, the physiological waveforms transmitted by the *BioHarness 3*, and other, wireless sensors are not without their faults. Various noise artefacts can significantly alter the data and provide the medical professionals, and other automated systems, with incomplete or potentially misleading data. To mitigate this problem, algorithms are needed to continuously monitor this large volume of data, detect artefacts, and inform medical professionals of their reliability.

Section 2 discusses the *BioHarness 3* sensor system in more detail followed by an explanation of the various artefact sources. A set of criteria are developed in Section 3 to evaluate different artefact detection algorithms, and help developers and researchers compare various sensor systems with the aim of automatically accumulating physiological data for both automated analysis. In the next secion, a series of artefact identification and filtering algorithms are then examined, tested and evaluated using these selection criteria. These help to ensure that the data collected is both consistent and reliable to provide a practical medical diagnosis value.

2. Sensor Characteristics: The *BioHarness 3* provides three sensors: an accelerometer, electrocardiography (ECG) sensor and respiration sensor. Each sensor is recorded independently and transmitted to the patient's smartphone in distinct packets using *Bluetooth*. Within the smartphone (base station), the data is filtered and collated before being sent onwards through the system. The combined data rate is approximately 5 kb/s and is recorded in two minute bursts every ten minutes to provide sufficient battery life for continuous wear.

The tri-axial accelerometer provides three channels at 50 Hz corresponding to the Cartesian coordinates from the belt. The respiration sensor is a single-band rib cage capacitive pressure plethysmography device, which can only provide a waveform

illustrating the expansion of the thoracic cavity but cannot quantify the size of the chest expansion. The ECG sensor provides a 250 Hz signal similar to second modified lead on a traditional non-portable ECG device. This signal is a downsampled recording of the 1 kHz sample rate achieved by the sensor. Access to all of these data signals can be unreliable at times due to the artefacts, discussed in the next section.

3. Artefacts:

3.1. Selection Criteria: To identify the algorithms required for eliminating ECG artefacts, their potential causes are investigated. Table 1 outlines five possible artefacts that have been explored [4], including the style of noise introduced by these artefacts.

Table 1 Frequency ranges of common ECG artefacts.

Artefact	Noise Introduced	Cause
Drift	0.5 Hz Sine wave	Breathing
Motion	5 Hz Sine wave	Body motion
Mains	50 Hz Sine wave	Electrical interference
Electromyography	Random noise	Muscle movement
Attenuation	Low SNR	Poor sensor placement

A naïve artefact filtering algorithm may discard any signals that fall out of the frequencies of interest. However one purpose of the system proposed here, to monitor patients with diabetes, is to help medical professionals diagnose potential heart problems. Diagnosing an abnormal ECG signal may require the entire unmodified waveform for analysis. As an example, a standard high-pass filter applied to the electrocardiogram waveform can cause phase shifts which distort the ST segment of the waveform [5]. Therefore careful selection of the algorithms used to enhance the legibility of the waveforms is critical.

The frequencies of interest for ECG waveforms can be seen in the power spectral density (PSD) plot of an ideal synthetic ECG waveform [6] in Fig. 1. The energy within the signal is contained mostly between the 5–40 Hz range, however other details that can assist with diagnosis may be hidden amongst the aliasing artefacts shown within this plot. Therefore this frequency range can be taken as a comparative metric, but care must be taken because the QRS complex within the ECG can be composed of some higher frequencies up to 100 Hz [7].

4. Comparison Methodology:

In order to compare different algorithms for artefact detection, the following metrics are used to assess their usefulness, performance and computation requirements.

4.1. Signal Quality: This is used to establish the useful power within the signal in order to investigate whether a filter algorithm has successfully removed the energy from artefacts. It is important to see whether the frequencies of most interest have been enhanced or attenuated by the artefact filter under test. Adapted from existing research [9] and applied to mHealth, two signal quality metrics are investigated to analyse the power of the ECG data produced by a sensor in certain frequency bands.

The baseline power metric, shown in Eq. (1) compares the power in the main area of interest (0–40 Hz) to the power primarily associated with baseline noise, frequently caused by breathing artefacts that occur around 0.5 Hz [4]. Its result is a number between zero and one that corresponds to the useful power in the signal. A high value indicates that the signal contains data of interest, whereas a low value corresponds to faulty or incomplete data.

$$\mathrm{basSQI} = 1 - \left(\frac{\int_0^1 P(f)\mathrm{d}f}{\int_0^{40} P(f)\mathrm{d}f} \right) \tag{1}$$

Another important aspect of the ECG waveform is the QRS complex which has power contained within a certain frequency band. The relative power in this part of the waveform needs to be examined as well to ensure the reliability of the ECG waveform. This is computed using the relative power ratio shown in Eq. (2). As before, a high value of pSQI indicates that data of interest is present, while a low value corresponds to erroneous data. Artefacts such as the baseline noise caused by breathing, muscle contractions and general body motion all occur below 5 Hz [10]. Therefore this equation aims to test the successfulness of any filtering algorithm.

$$\mathrm{pSQI} = \frac{\int_5^{15} P(f)\mathrm{d}f}{\int_5^{40} P(f)\mathrm{d}f} \tag{2}$$

4.2. Interpretation Quality: A key use of the ECG waveform is to analyse the intervals between the main peaks within the signal to establish the heart rate of the patient in beats per minute. Therefore, the interpretation quality metric investigates whether the resulting waveform is corrupted by the algorithm under test, and whether this may lead to a misdiagnosis. To assess this, 16 records from the *MIT-BIH Arrhythmia Database* [11] were adapted for analysis. These records were from normal patients using standard hospital ECG recording apparatus. Only records with complete *MLII* (second modified lead) waveforms were considered for use, as this closely replicates the waveform recorded by the *BioHarness 3* with its single lead. A cardiologist hand inspected each waveform, counting the number of QRS complexes within it. This was compared to a count produced using the *Open Source ECG Analyser* (*OSEA*) [8] which is known to perform well with portable dry electrodes [12]. Records where the *OSEA* QRS complex count was not within 99.5% of the cardiologist's count were discarded, leaving 16 records.

Algorithms that impede the automatic interpretation of conditions, such as Arrhythmias, should not be used in mHealth systems. Therefore the interpretation quality metric defined here provides a basic method of comparison to select filtering algorithms that impede interpretation the least.

4.3. Computational Complexity: Due to the constrictive programming environment within most smartphone application platforms and sensor nodes, the ability to determine the computational complexity is not precise. Therefore the standard *big-O* notation will be utilised to examine each algorithm, as this metric remains consistent between most programming languages and is a suitable way of comparing algorithms. *Big-O* explains the complexity associated with an algorithm by defining the mathematical function that limits it.

5. Identification and Filtering Algorithms:

Performing the artefact identification and filtering on the base station itself permits both patients and developers to utilise the sensors of their choice without the hospital side of the system requiring modification. Therefore reducing the computational complexity of the identification algorithms is important. Another aspect of the filtering is the necessity to not alter the resulting waveforms that are transmitted through the system. The potential for misdiagnosis, particularly when detecting heart abnormalities is critical in an unsupervised mHealth environment.

Consequently, a series of low-complexity algorithms are designed and implemented to consume as few resources as possible to enhance battery life and performance within a resource constrained device. These are further investigated and tested against the three metrics previously described for signal quality, interpretation quality and computational complexity.

Each algorithm targets a particular kind of artefact. Hence, in order to better evaluate the efficiency of each technique a synthetic ECG signal is firstly used with one specific artefact superimposed

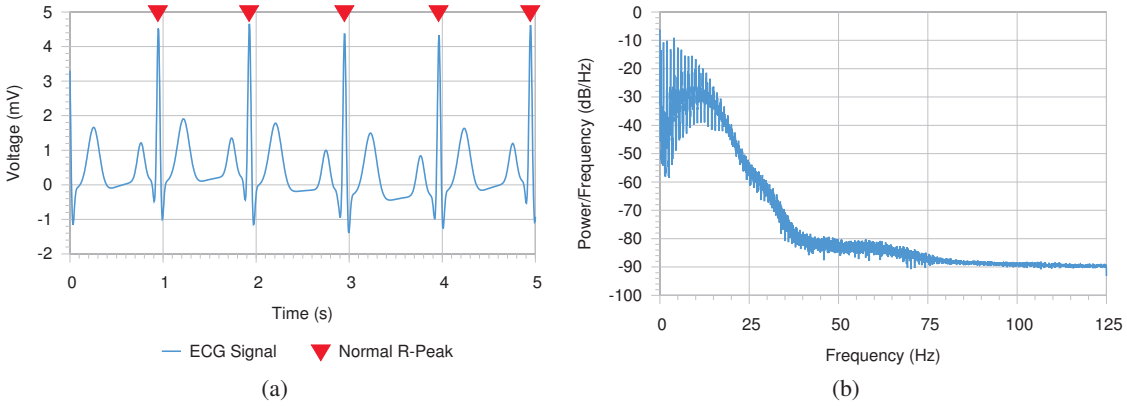

Figure 1 *(a)An arbitrary five second segment of an synthetic ECG waveform with no artefacts. The red diamonds indicate R-peaks detected using the OSEA algorithm [8]; (b) The power spectral density of a synthetic ECG waveform with no added artefacts*

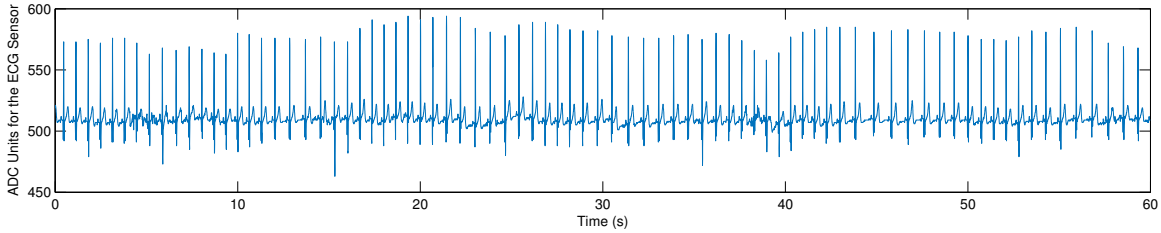

Figure 2. An ECG signal obtained using the BioHarness 3.

on to it. A real signal such as the one shown in Fig. 2, obtained using the *BioHarness 3* sensor, simultaneously has more than one artefact added to it. However, illustrative values for the different metrics are nonetheless also calculated for real ECG acquired using the *BioHarness 3* sensor in bursts of 120 seconds.

5.1. Saturation Artefacts: There can be a number of reasons for saturation artefacts e.g. large body movements. These are ultimately the result of improper gain selection on the sensor. Since the gain is not user configurable on most domestic ECG sensors such as the *BioHarness 3*, the possibility of such artefacts occurring is high enough to warrant identification. The corruption to the waveform caused by these artefacts cannot be filtered, and therefore the signal must be identified as containing an artefact.

A standard packet-based threshold algorithm for identifying saturation is explored, where the thresholds were observed by manual inspection of the device. If any one sample within a packet of 63 samples crossed either of these thresholds, the entire packet was marked as saturated to encapsulate the gradual rise or fall to one of the limits. The results of this algorithm are demonstrated in Fig. 3 in a similar manner to the interface provided to medical professionals as part of the entire patient monitoring system.

Two further saturation identification algorithms were explored: the rail contact mask [13] and Analogue-to-Digital Converter (ADC) clipping [14]. The rail contact mask [13] identifies a whole second of samples if they exist within 1% of the limits of the ADC resolution. The ADC clipping algorithm [14] identifies a second of data (e.g. a single R-peak interval at a common heart rate of 60 beats per minute) as an artefact should two consecutive samples lie beyond 95% of the average signal amplitude.

Both of these algorithms identify artefacts without filtering data, therefore the comparison criteria are not suited for this class of artefact. The complexity of these algorithms is $O(n)$, as they only operate on the input waveform to conduct static comparisons.

5.2. Mains Artefacts: Occasionally ungrounded sensors can receive mains wiring noise through their inputs. This form of

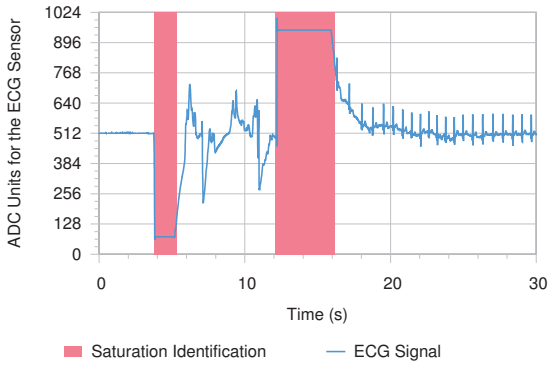

Figure 3 *An example ECG waveform recorded by the BioHarness 3 showing the output of the original saturation identification algorithm.*

artefact does not affect the accelerometer or respiration sensors because the common mains frequencies of 50 Hz and 60 Hz occur beyond their range of interest. However, it does affect ECG signals since they contain important information around these frequencies. This artefact is difficult to observe on the real ECG obtained from the *BioHarness 3* (Fig. 2) due to the presence of other artefacts. To emphasize the effect of this artefact alone, Fig. 4(a) shows a synthetic ECG waveform at 60 beats per minute, with a 14 dB 50 Hz sinusoidal signal added. Removing this would significantly increase the legibility of the QRS complex, although the *OSEA* algorithm [8] can still extract the R-peak interval despite this noise.

In the European Union, all mains electrical supplies are standardised at a frequency of 50 Hz permitted to vary by 200 mHz [15]. As shown in Fig. 4(b), the PSD of a synthetic ECG waveform with 20% mains noise causes a very large spike at 50 Hz. A common method of removing this power spike is to use a notch filter [16] with a second order IIR filter being a frequent implementation [7], [13]. Such a filter on the ECG waveform is known not to produce appreciable distortion [17], and

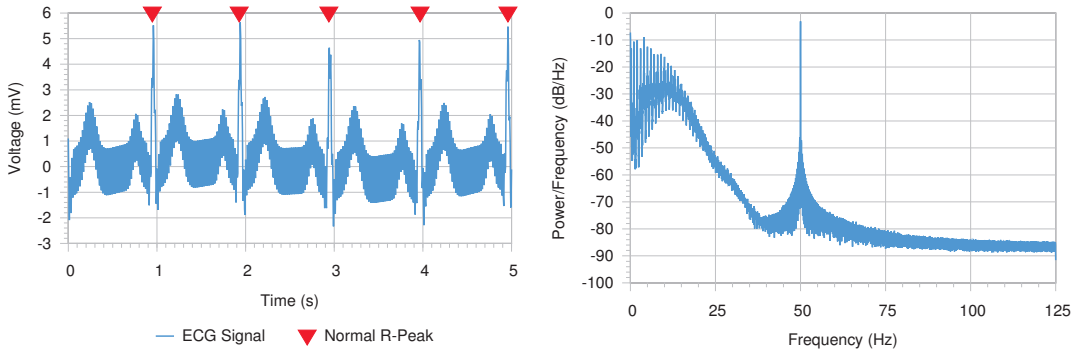

(a) (b)

Figure 4 *(a)An arbitrary five second segment of an synthetic ECG waveform with an added mains artefact at a typical 14 dB. The red diamonds indicate R-peaks detected using the OSEA algorithm [8]; (b) The power spectral density of a synthetic ECG waveform with an added mains artefact.*

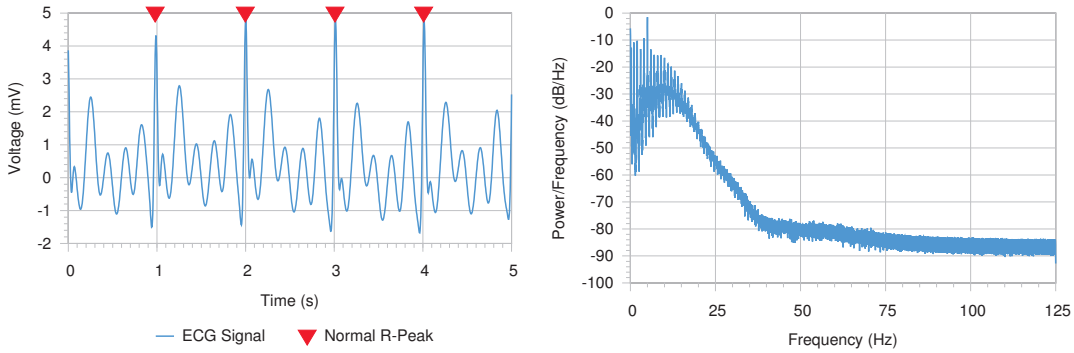

(a) (b)

Figure 5 *(a) An arbitrary five second segment of an synthetic ECG waveform with an added movement artefact. The red diamonds indicate R-peaks detected using the OSEA algorithm [8]; (b) The power spectral density of a synthetic ECG waveform with an added movement artefact.*

this is reflected in the signal quality indices, which do not alter regardless of the percentage of mains noise added, and regardless of the average heart rate of the synthetic ECG. For an ECG recorded by the *BioHarness 3* with a heart rate of 72 beats per minute, the baseline power is improved by over 9%. For a synthetic ECG signal with 120 beats per minute, the potential improvement is 10%. There is no alteration in the relative power for both real or synthetic signals in the QRS complex, because the noise from the mains does not occur in the range under question. With the interpretation quality metric, no interference was observed with the identification of R-peaks by the *OSEA* algorithm regardless of heart rate or mains noise amplitude. However, this finding is due to algorithm's ability to compensate for this type of noise [8]. Finally, the computational complexity of the mains filter is $O(n^2)$ because of the type of array indexing required by the digital filter. Such a filter can be computationally expensive, however the floating-point performance of most modern smartphones is sufficient for such processing.

5.3. Involuntary Movement Artefacts: These are usually caused by the involuntary muscle contractions and can be observed as high amplitude spikes in the 0–5 Hz range [12]. Typical advice for professional non-ambulatory ECG recording include raising the room temperature to reduce shivering and other muscular movements. The effect of these movements can be seen on real ECG signals around 5-second and 38-second mark on Fig. 2. Although it appears to be small corruption of the signal the effect of the movement artefact is significant in interpreting the ECG. Fig. 5(a) highlights this on a synthetic ECG waveform where the the QRS complex is not legible as a result of adding movement artefacts. This distortion is evident by the peak in the PSD at 5 Hz as shown in Fig. 5(b). Ghasemzadeh *et al.* [18] evaluated several motion artefact filters, however there is no clear conclusion available due to the noise being too similar to the ECG signal. Further, such algorithms frequently remove useful data which is critical for medical professionals.

5.4. Drift Artefacts: Baseline drift artefacts on the ECG waveform are frequently caused by breathing, however a correlation cannot be assumed because such artefacts are also associated with poor sensor placement thus invalidating both signals [19].

Fig. 2 shows the effect of baseline drift artefact on ECG signal acquired using the *BioHarness 3* between 20 and 30 seconds on time axis. While there are amplitude changes, the details of the waveform still appear legible. This is further shown using a synthetic ECG signal in Fig. 6(a). A filtering method, such as the Discrete Wavelet Transform [20], can be used to produce a corrected waveform, however this can corrupt the original signal which is important for the detection of heart abnormalities [18], [21]. The PSD of the synthetic ECG signal, in Fig. 6(b), shows that the spectrum is broadly unchanged from the unaltered synthetic waveform, highlighting the difficulties in removing low frequency components of the signal which is similar to the noise distribution.

Two algorithms for removing baseline drift artefacts, based upon median filtering, are explored to avoid any potential distortions and keeping the computational complexity low. The first one is a simple median filter [18] that applies a median operator to a window of half the sample rate. The second one is a mean-median filter [21] which combines both a mean and a median operator to the same sized window to better remove the non-linear artefacts.

The two algorithms result in no corruption to the relative power in the QRS complex of the unfiltered ECG. Further, the interpretation quality is not compromised since all the R-peaks, in both synthetic and real ECG signals, were identified after applying the two filters. The results were consistent at differing amounts of added

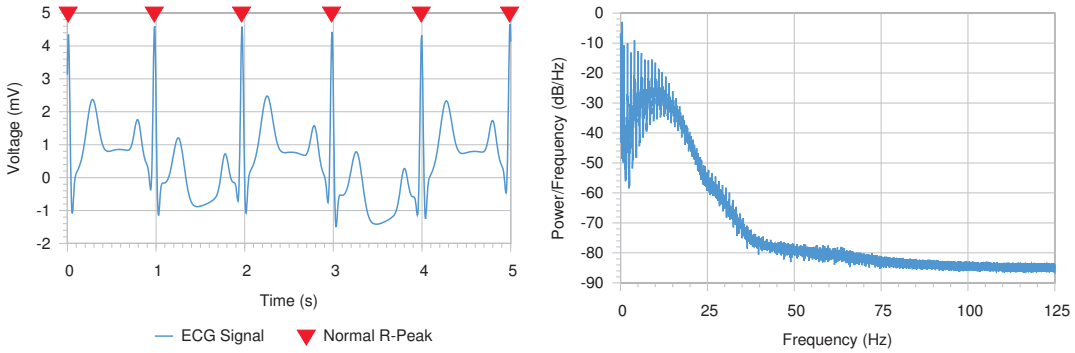

Figure 6 *(a) An arbitrary five second segment of an synthetic ECG waveform with an added baseline drift artefact at a typical 14 dB. The red diamonds indicate R-peaks detected using the OSEA algorithm [8]; (b) The power spectral density of a synthetic ECG waveform with an added baseline drift artefact.*

baseline drift noise suggesting no significant alterations to the ECG waveform. Improvements of up to 24% in the relative power of the baseline were observed when using the mean-median filter, compared to 13% for the median filter with an ECG signal acquired using the *BioHarness 3*. These improvements were even higher for a synthetic ECG signal at 29% and 16% for the mean-median and median filters respectively. The baseband power index (basSQI), using the real ECG signal, increased from an average of 0.217 to 0.979, indicating a much more useful signal when the two filters were used. The computational complexity of both filters is also relatively simple at $O(\log n)$.

5.5. Low Signal-to-Noise Ratio (SNR): Low SNR artefacts commonly occur due to breathing or poor sensor placement. They disrupt the incoming waveform and therefore no filtering is possible to rectify the signal. A common implementation of an identification algorithm to remove this noise uses hugely complex series of filters such as the low power mask algorithm [13]. However, this is not suitable for low-power implementation due to its complexity and may also distort the ECG waveform. A simpler solution is to maintain the current low SNR criterion which utilises a static threshold to determine whether the amplitude of a sample window was sufficient to be interpreted as a valid signal.

For ECG signals, a minimum SNR of 20 dB is the clinically accepted standard [22] for the analysis of the QRS complex. Therefore a range of 10% of the input resolution should be used as the criteria for detecting unacceptable levels of noise and hence flag this to the medical professional to indicate that the data they are observing might be unreliable. An example of this artefact identification flag can be seen in Fig. 7, where an ECG waveform recorded by the *BioHarness 3* has been artificially attenuated for a set duration to demonstrate the algorithm.

The computational complexity of such an algorithm is $O(n)$ in the time domain, because of the static comparison.

6. Discussion: To continue providing consistent and reliable sensor data to medical professionals, there is a need to identify artefacts automatically and clean this data before transmitting. Further, in cases where it is not possible to filter data properly the doctors should have access to the raw data. The dataflow from the sensors to the transmitted data with inermediate artefact identification is depicted in Fig. 8. The physiological sensor data is parsed through the previously mentioned artefact identification and filters to produce filtered data. In addition, should any artefacts identification or filter algorithm detect that the SNR of the waveform is less than 20 dB, then the relevant noise flags will be recorded and the unfiltered data will be sent from the patient's smartphone to the database server and automated analysis engine.

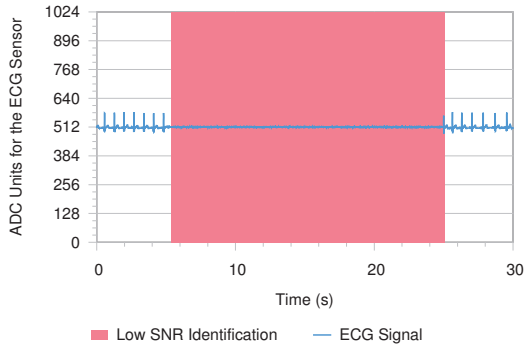

Figure 7 *An ECG waveform recorded by the BioHarness 3 showing the output of the original low signal-to-noise ratio identification algorithm.*

The artefact filter algorithms to remove baseline drift and mains interference are only executed if the noise is less than 10% of the signal amplitude. The baseline drift, low SNR, mains interference and saturation identification algorithms are combined so that if any one algorithm identifies an artefact, the relevant packets transmitted by the *BioHarness 3* are flagged as such, and the unfiltered data is transmitted to the server. This dataflow provides the doctors with reliable data in the best case scenario, where the artefacts are minimal, and some noisy data in the worst case scenario.

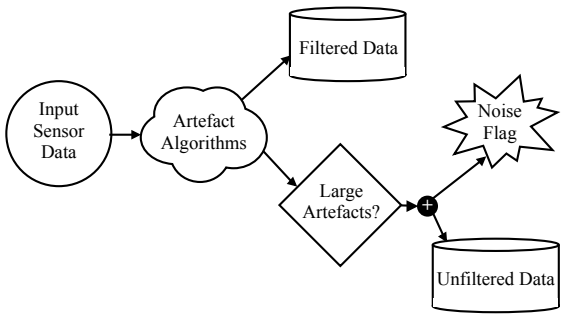

Figure 8. Dataflow for continous long-term recording of sensor data.

The signal quality metrics described in this paper can be used to interpret the effectiveness of certain artefact removing algorithms both in terms of the quality of the signal as well as the computational efficiency of the algorithm. Other methods proposed in literature to assess ECG signal quality include algorithms to detect flatness, impulses and Gaussian noise within the signal [23]. Since the ECG signal is bounded, its dynamic range can also be

used to interpret its signal quality [24]. Additionally, the signal may also be quantified by estimating the average beat quality [25]. Orphanidou *et al.* [26] proposed checking for heart rate and RR interval to determine if they fall within a normal range. They also performed template matching to ensure most properties of the ECG signal were preserved. Apart from those covered in this paper, there are many other artefacts as well that can degrade the quality of an ECG signal. More metrics and algorithms to address them are needed, particularly for sensors used in the context of mHealth.

7. Conclusion: Continuous monitoring of patients is a pivotal part of mHealth, and one which still warrants further research. While the artefact detection and filtering algorithms described here are not the best available, they do satisfy the metrics described previously to determine the suitability for an algorithm in a mHealth environment. Signal quality, interpretation quality and computation complexity each reflect the requirements placed on ubiquitous sensor networks when used in a healthcare scenario. The aim of the artefact identification algorithms described is to make the absolute best use of the sensor data, and to assist both medical professionals in their interpretation of the data and the patients themselves—to ensure that unsupervised recording is working sufficiently well. It is hoped that the metrics and algorithms described in this paper can be useful for designers of mHealth systems and help them to collect reliable data with true diagnostic value.

8. Funding and Declaration of Interests: This work was partially supported by the EU FP7 project *Commodity12*.

9 References

[1] Ö. Kafalı, S. Bromuri, M. Sindlar, T. van der Weide, E. A. Pelaez, U. Schaechtle, B. Alves, D. Zufferey, E. Rodriguez-Villegas, M. I. Schumacher, and K. Stathis, "Commodity12: A smart e-health environment for diabetes management," *J Ambient Intell Smart Environ*, vol. 5, no. 5, pp. 479–502, 2013.

[2] M. Safford, L. Russell, D. Suh, S. Roman, and L. Pogach, "How much time do patients with diabetes spend on self-care," *J Am Board Fam Pract*, vol. 18, no. 4, pp. 262–270, 2005.

[3] Zephyr Technology Corporation. (2016) BioHarness 3. [Online]. Available: http://www.zephyranywhere.com/products/bioharness-3.

[4] A. Ruha, S. Sallinen, and S. Nissilä, "A real-time microprocessor qrs detector system with a 1-ms timing accuracy for the measurement of ambulatory hrv," *IEEE Trans Biomed Eng*, vol. 44, no. 3, pp. 159–167, 1997.

[5] F. Buendia-Fuentes, M. A. Arnau-Vives, A. Arnau-Vives, Y. Jimenez-Jimenez, J. Rueda-Soriano, E. Zorio-Grima, A. Osa-Saez, L. V. Martinez-Dolz, L. Almenar-Bonet, , and M. A. Palencia-Perez, "High-bandpass filters in electrocardiography: Source of error in the interpretation of the st segment," *ISRN Cardiology*, 2012.

[6] P. E. McSharry, G. D. Clifford, L. Tarassenko, and L. A. Smith, "A dynamical model for generating synthetic electrocardiogram signal," *IEEE Trans Biomed Eng*, vol. 50, no. 3, pp. 289–294, 2003.

[7] M. S. Chavan, R. A. Agarwala, , and M. D. Uplane, "Digital FIR equiripple notch filter on ECG signal for removal of power line interference," *WSEAS Trans Signal Processing*, vol. 4, no. 4, pp. 221–230, 2008.

[8] P. S. Hamilton - E. P. Limited. (2016) Open Source ECG Analysis Software Documentation. [Online]. Available: http://www.eplimited.com/.

[9] G. D. Clifford and G. B. Moody, "Signal quality in cardiorespiratory monitoring," *Physiol Meas*, vol. 33, no. 9, 2012.

[10] G. D. Clifford, F. Azuaje, and P. McSharry, *Advanced Methods and Tools for ECG Data Analysis*. Artech House, 2006.

[11] A. L. Goldberger, L. A. N. Amaral, L. Glass, J. M. Hausdorff, P. C. Ivanov, R. G. Mark, J. E. Mietus, G. B. Moody, C.-K. Peng, and H. E. Stanley, "PhysioBank, PhysioToolkit, and PhysioNet: Components of a new research resource for complex physiologic signals," *Circulation*, vol. 101, no. 23, pp. e215–e220, 2000.

[12] J. Ottenbacher and M. Kirst, "Reliable motion artifact detection for ECG monitoring systems with dry electrodes," in *IEEE EMBC*, Vancouver, August 2008.

[13] S. J. Redmond, N. H. Lovell, J. Basilakis, and B. G. Celler, "ECG quality measures in telecare monitoring," in *IEEE EMBC*, Vancouver, August 2008.

[14] G. D. Fraser, A. D. C. Chan, J. R. Green, and D. MacIsaac, "Detection of ADC clipping, quantization noise, and amplifier saturation in surface electromyography," in *IEEE MeMeA*, Budapest, May 2012.

[15] ENTSO-E. (2013) Network code on load-frequency control and reserves. [Online]. Available: https://www.entsoe.eu/.

[16] S. V. Vaseghi, *Multimedia Signal Processing: Theory and Applications in Speech, Music and Communications*. Wiley, 2007.

[17] A. S. Vale-Cardoso and H. N. G. aes, "The effect of 50/60 hz notch filter application on human and rat ecg recording," *Physiol Meas*, vol. 31, no. 1, pp. 45–58, 2010.

[18] H. Ghasemzadeh, S. Ostadabbas, S. Member, E. Guenterberg, and A. Pantelopoulos, "Wireless medical-embedded systems : A review of signal-processing techniques for classification," *IEEE Sensors*, vol. 13, no. 2, pp. 423–437, 2013.

[19] K. Pandia, S. Ravindran, R. Cole, G. Kovacs, and L. Giovangrandi, "Motion artifact cancellation to obtain heart sounds from a single chest-worn accelerometer," in *IEEE ICASSP*, Boston, March 2010.

[20] R. von Borries, J. Pierluissi, and H. Nazeran, "Wavelet transform-based ECG baseline drift removal for body surface potential mapping," in *IEEE EMBC*, Shanghai, September 2005.

[21] W. Hao, Y. Chen, and Y. Xin, "ECG baseline wander correction by mean-median filter and discrete wavelet transform," in *IEEE EMBC*, Boston, September 2011.

[22] R. E. Herrera, J. T. Cain, E. Capet, and G. J. Boylel, "A high resolution ECG tool for detection of atrial and ventricular late potentials," in *Computers in Cardiology*, Indianapolis, September 1996.

[23] C. Liu, P. Li, L. Zhao, F. Liu, and R. Wang, "Real-time signal quality assessment for ecgs collected using mobile phones," in *2011 Computing in Cardiology*, September 2011.

[24] B. E. Moody, "Rule-based methods for ecg quality control," in *2011 Computing in Cardiology*, September 2011.

[25] L. Johannesen, "Assessment of ecg quality on an Android platform," in *2011 Computing in Cardiology*, September 2011.

[26] C. Orphanidou, T. Bonnici, P. Charlton, D. Clifton, D. Vallance, and L. Tarassenko, "Signal-quality indices for the electrocardiogram and photoplethysmogram: Derivation and applications to wireless monitoring," *IEEE J Biomed Health Inform*, vol. 19, no. 3, pp. 832–838, 2015.